Supporting Information

Interligand Communication in a Metal Mediated LL'CT System – A Case Study

Sara A. Dille,[a] Kyle J. Colston,[a] Stephen C. Ratvasky,[b] Jingzhi Pu,[a] and Partha Basu*[a]

[a]   Dr. S. A. Dille, Mr. K. J. Colston, Dr. J. Pu, and Dr. P. Basu
        Department of Chemistry and Chemical Biology
        Indiana University – Purdue University Indianapolis
        Indianapolis, IN, 46202, USA
        E-mail: basup@iupui.edu
[b]   Mr S. C. Ratvasky
        Department of Chemistry and Biochemistry
        Duquesne University
        Pittsburgh, PA, 15282, USA

Experimental Section

Materials. All reagents and solvents were purchased from either Sigma Aldrich or Thermo Fisher Scientific and used as received without further purification. All work was carried out under an inert atmosphere either in a dry box or using Schlenk line techniques under argon. $[MoOCl(^iPr_2Dt^0)_2][PF_6]$, $[MoOCl(Me_2Dt^0)_2][PF_6]$[12], *N,N'*-diisopropylpiperazine-2,3-dithione ($^iPr_2Dt^0$), and *N,N'*-dimethylpiperazine-2,3-dithione (Me_2Dt^0)[60] were synthesized following literature procedures. Multivariate regression analyses for Kamlet-Taft models were performed using Minitab 18 software.

Physical Methods. ^1H NMR spectra were recorded on either a Bruker 500 MHz Avance spectrometer or a Bruker 400 MHz Avance spectrometer in air-tight NMR tubes.^{31}P NMR spectra were recorded on a Bruker 400 MHz Avance spectrometer in air-tight NMR tubes. Infrared spectroscopy (FTIR) was recorded using a Thermofisher Nicolet iS10 spectrometer at room temperature using a KBr pellet. Electronic absorbance spectra were collected on a Shimadzu UV-3600 Plus in an air tight quartz cuvette. Cyclic voltammetry was recorded on a Metrohm PGSTAT204 galvanostat/potentiostat. A Pt disk working electrode, Ag^+/Ag reference electrode and Pt wire auxillary electrode and tetrabutylammonium hexafluorophosphate supporting electrolyte were used. All voltammograms were referenced to the Fc^+/Fc couple as an internal standard. All potentials are presented versus the Fc^+/Fc couple, Mass spectra were collected using an Agilent Technologies 6520 Accurate Mass-QTOF LC/MS.

Computational Methods. All computational work was performed using *Gaussian 09* software package running on UNIX OS and visualized utilizing *GaussView 5.0.9*.

Calculations were done using the Lee-Yang-Parr nonlocal correlation functional[61] (B3LYP) and a combination of the LANL2DZ[62] effective core potential basis set for molybdenum and the 6-31G** basis set for all other atoms. The crystal structure geometry was optimized using DFT to afford the geometry used for subsequent calculations. Atomic composition for molecular orbitals was determined using C-squared population analysis from single-point calculations with the program *QM-Forge*. The lowest 60 transition energies were generated using non-equilibrium TDDFT calculations with the polarizable continuum model (PCM) algorithm. PCM-TDDFT calculations were performed using acetonitrile as the solvent to match experimental conditions. Electron density difference maps (EDDMs) were generated using the *cubman* package in *Gaussian09*.

X-Ray Crystallography. Single crystals were mounted using glass fiber and data collected using a Bruker SMART Apex II diffractometer with a graphite monochromator for Mo Kα radiation (0.71073 Å). The absorption correction was performed using SADABS routine.[63] The structure solution and the refinement were done using SHELXS-97[64] and SHEXLX-2018 programs.[65] The X-ray data were collected at room temperature (296 K). Hydrogen atoms were placed at calculated positions and refined as riding atoms with isotropic displacement parameters. The methyl group on the toluene-2,3-dithiolene moiety of MoO(tdt)(^{i}PrDt^{0}) was refined as disordered over two moieties with different rotational orientations. The disorder extends to the other carbon and sulfur atoms of the toluene-2,3-dithiolene moiety, and they were included in the disorder modeling. The two moieties were restrained to have similar geometries (SAME command of Shelxl) and U_{ij} components of ADPs for disordered atoms closer to each other than 2.0 Angstrom were restrained to be

similar. Subject to these conditions, the occupancy ratio refined to 0.517(5) to 0.483(5).

Details of the structure determination are listed in Table S1.

Table S1. Crystallographic Data for MoO(tdt)(^{i}Pr$_2$Dt^0)

Formula	C$_{17}$H$_{24}$MoN$_2$OS$_4$
Formula weight	496.56
Temperature	296 K
Color/shape	Purple/Block
Crystal system	Orthorhombic
Space group	Pbca
	a=12.6981 (1) Å
Unit cell dimensions	b= 15.8799 (2) Å
	c= 21.2754 (2) Å
Volume (Å^3)	4290.07(8)
Z, Formula unit/unit cell	8
density (calculated)	1.534 Mg m^{-3}
μ (mm^{-1})	1.01
Diffractometer	Bruker Smart Apex II
Radiation, graphite monochrome	Mo Kα (λ=0.71073 Å)
Crystal size	0.20 x 0.11 x 0.08 mm
Reflections collected/unique	70727/6665
Parameters/restraints	314/292
R$_{int}$	0.054
Refinement method	Full-matrix least-squares on F^2
Goodness-of-fit on F^2	1.03
Final R indices [I>2σ(I)]	R=0.041 wR2=0.100
Maximum residue peaks (e·Å^{-3})	0.53 and -0.44

Syntheses of Complexes

MoO(bdt)(Me$_2$Dt^0) (1). [MoOCl(Me$_2$Dt^0)$_2$][PF$_6$] (200 mg, 0.312 mmol) was dissolved in 9 mL of acetonitrile generating a dark blue solution. A solution of benzenedithiol (63 mg, 0.34 mmol) and triethylamine (69 mg, 0.68 mmol) in 1.5 mL of acetonitrile was added dropwise to the dark blue solution initiating an instantaneous color change to dark purple and the release of white vapor. The reaction mixture was stirred for one hour. The solution was filtered, and dark purple solid was collected. The crude product was washed with cold chloroform to obtain analytically pure product. Yield 56% (75 mg, 0.175 mmol). Calcd (Expt) for C$_{12}$H$_{14}$MoN$_2$OS$_4$: C, 33.80 (33.95): H, 3.31 (3.34); N, 6.33 (6.57). ^{1}H NMR (CD$_3$CN): δ 3.77 (s, CH$_3$, 6H), 3.89 (m, CH$_2$, 2H), 4.18 (m, CH$_2$, 2H), 7.10 (dd, J= 5.8 Hz, 3.2 Hz, aromatic, 2H), 7.65 (dd, J= 5.8 Hz, 3.2 Hz, aromatic, 2H). FTIR (KBr, cm^{-1}): 1531 (vs, C(-N)S), 1354 (vs, C=S), 940 (s, Mo=O). UV-Vis (MeCN): λ$_{max}$ (ε, M^{-1}cm^{-1}) 380 nm (1610), 532 nm (4400).

MoO(tdt)(Me$_2$Dt^0) (2). [MoOCl(Me$_2$Dt^0)$_2$][PF$_6$] (200 mg, 0.312 mmol) was dissolved in 9 mL of acetonitrile generating a dark blue solution. A solution of toluene-3,4-dithiol (53 mg, 0.34 mmol) and triethylamine (69 mg, 0.68 mmol) in 1.5 mL of acetonitrile was added dropwise to the dark blue solution initiating an instantaneous color change to dark purple and the release of white vapor. The reaction mixture was stirred for one hour. The solution was filtered and dark purple solid was collected. The crude product was washed with cold chloroform to obtain analytically pure product. (79 mg, 0.164 mmol). 52% Calcd (Expt) for C$_{13}$H$_{16}$MoN$_2$OS$_4$: C, 35.45 (35.44): H, 3.66 (3.74); N, 6.36 (6.24). ^{1}H NMR (CD$_3$CN): δ 2.34 (s, CH$_3$, 3H), 3.76 (s, CH$_3$, 6H), 3.86 (m, CH$_2$, 2H), 4.14 (m,

CH$_2$, 2H), 6.92 (d, J= 7.87 Hz, aromatic 1H), 7.47 (s, aromatic, 1H), 7.51 (d, J= 7.9 Hz, aromatic, 1H). FTIR (KBr, cm^{-1}): 1534 (vs, C(-N)S), 1355 (vs, C=S), 929 (s, Mo=O). UV-Vis (MeCN): λ_{max} (ε, M^{-1}cm^{-1}) 380 nm (2320), 531 nm (6050).

MoO(qdt)(Me$_2$Dt^0) (3). [MoOCl(Me$_2$Dt^0)$_2$][PF$_6$] (200 mg, 0.312 mmol)was dissolved in 9 mL of acetonitrile generating a dark blue solution. A solution of qunioxalinedithiol (66 mg, 0.34 mmol) and triethylamine (69 mg, 0.68 mmol) in 1.5 mL of acetonitrile was added dropwise to the dark blue solution initiating an instantaneous color change to dark purple and the release of white vapor. The reaction mixture was stirred for one hour. The solution was filtered and dark purple solid was collected. The crude product was washed with cold chloroform to obtain analytically pure product. (20 mg, 0.0401 mmol). 11% Calcd (Expt) for C$_{14}$H$_{14}$MoN$_4$OS$_4$ +H$_2$O: C, 33.87(34.21): H, 3.25(2.82); N, 11.28 11.84). ^{1}H NMR (CD$_3$CN): δ 3.84 (s, CH$_3$, 6H), 4.00 (q, J= 8.2 Hz, 7.0 Hz, CH$_2$, 2H), 4.21(q, J= 7.0 Hz, 6.4 Hz, CH$_2$, 2H), 7.63 (dd, J= 6.4 Hz, 3.4 Hz, aromatic, 2H), 7.93 (dd, J= 6.4 Hz, 3.4 Hz, aromatic, 2H). FTIR (KBr, cm^{-1}): 1524 (vs, C(-N)S), 1350 (vs, C=S), 955 (s, Mo=O). UV-Vis (MeCN): λ_{max} (ε, M^{-1}cm^{-1}) 410 nm (6110), 548 nm (7450).

MoO(bdtCl$_2$)(Me$_2$Dt^0) (4). [MoOCl(Me$_2$Dt^0)$_2$][PF$_6$] (200 mg, 0.312 mmol) was dissolved in 9 mL of acetonitrile generating a dark blue solution. A solution of 3,6-dichloro-1,2-benzenedithiol (72 mg, 0.34 mmol) and triethylamine (69 mg, 0.68 mmol) in 1.5 mL of acetonitrile was added dropwise to the dark blue solution initiating an instantaneous color change to dark purple. The reaction mixture was stirred for thirty minutes. The solution was filtered and dark purple solid was collected. The crude product was washed with cold chloroform to obtain analytically pure product. Yield 42% (65 mg,

0.132 mmol). Calcd (Expt) for $C_{12}H_{12}Cl_2MoN_2OS_4$: C, 29.10 (29.35): H, 2.44 (2.50); N, 5.66 (5.69). ^{1}H NMR (CD$_3$CN): δ 3.81 (s, CH$_3$, 6H), 4.10 (m, CH$_2$, 2H), 4.20 (m, CH$_2$, 2H), 7.12 (s, aromatic 2H). FTIR (KBr, cm^{-1}): 1527 (vs, C(-N)S), 1353 (vs, C=S), 926 (s, Mo=O). Electronic spectrum, UV-Vis (MeCN): λ_{max} (ε, M^{-1}cm^{-1}) 385 nm (2050), 531 nm (4460).

MoO(bdt)(^{i}Pr$_2$Dt^0) (5). [MoOCl(^{i}Pr$_2$Dt^0)$_2$][PF$_6$] (200 mg, 0.26 mmol) was dissolved in 10.5 mL of acetonitrile generating a dark blue solution. A solution of benzenedithiol (49 mg, 0.34mmol) and triethylamine (59 mg, 0.58 mmol) in 1.5 mL of acetonitrile was added dropwise to the dark blue solution initiating an instantaneous color change to dark purple. The reaction mixture was stirred for one hour. The solution was filtered, and dark purple solid was collected. Free ^{i}Pr$_2$Dt^0 ligand was present in the crude product. To remove the free ligand, the crude product (80 mmol) was dissolved in 7.5 mL of CH$_3$Cl. MoCl$_5$ (10 mg, 0.037 mmol) was dissolved in 3 mL of MeOH generating HCl gas. The MoCl$_5$ was stirred until the cessation of the HCl gas was observed resulting in a green solution. The methanolic solution was added dropwise to the chloroform solution of the crude MoO(bdt)(^{i}Pr$_2$Dt^0). The mixture was stirred for 1.5 hours and filtered. A dark purple filtrate of analytically pure complex was collected. Yield 41% (52 mg, 0.107 mmol) Calcd (Expt) for $C_{16}H_{22}MoN_2OS_4$: C, 39.82 (40.24): H, 4.60 (4.51); N, 5.81 (5.54). ^{1}H NMR (CD$_3$CN): δ 1.28 (d, J= 6.7 Hz, CH$_3$, 6H), 1.43 (d, J= 6.7 Hz, CH$_3$, 6H), 3.74 (m, CH$_2$, 2H), 4.02 (m, CH$_2$, 2H), 5.23 (h, J= 6.7 Hz, CH, 2H), 7.10 (dd, J= 5.8 Hz, 3.2 Hz, aromatic, 2H), 7.65 (dd, J= 5.8 Hz, 3.3 Hz, aromatic, 2H) FTIR (KBr, cm^{-1}): 1501 (vs, C(-N)S), 1350 (vs, C=S), 931 (s, Mo=O). Electronic spectrum, UV-Vis (MeCN): λ_{max} (ε, M^{-1}cm^{-1}) 380 (2880), 529 nm (6900).

MoO(tdt)(^{i}Pr$_2$Dt^0) (6). [MoOCl(^{i}Pr$_2$Dt^0)$_2$][PF$_6$] (200 mg, 0.26 mmol) was dissolved in 9 mL of acetonitrile generating a dark blue solution. A solution of toluene-3,4-dithiol (0.45 g, 0.00029 moles) and triethylamine (59 mg, 0.58 mmol) in 1.5 mL of acetonitrile was added dropwise to the dark blue solution initiating an instantaneous color change to dark purple. The reaction mixture was stirred for one hour. The solution was filtered and dark purple solid was collected. The crude product was washed with cold chloroform resulting in analytically pure product. Yield 58% (77 mg, 0.155 mmol). Calcd (Expt) for C$_{17}$H$_{24}$MoN$_2$OS$_4$: C, 41.12 (41.04): H, 4.87 (4.76); N, 5.64 (5.52). ^{1}H NMR (CD$_2$Cl$_2$): δ 1.24 (d, CH$_3$, J= 6.9 Hz ,6H), 1.43 (d, J= 6.8 Hz, CH$_3$, 6H), 2.34 (s, CH$_3$, 3H), 3.62 (m, CH$_2$, 2H), 3.88 (m, CH$_2$, 2H), 5.22(h, J= 6.7 Hz, CH, 2H), 6.93 (d, J=8.1 Hz, aromatic H), 7.47 (s, aromatic, H), 7.51 (d, J= 7.9 Hz, aromatic, H). FTIR (KBr, cm^{-1}): 1501 (vs, C(-N)S), 1350 (vs, C=S), 931 (s, Mo=O). UV-Vis (MeCN): λ$_{max}$ (ε, M^{-1}cm^{-1}) 380 (2880) 533 nm (7500).

MoO(qdt)(^{i}Pr$_2$Dt^0) (7). [MoOCl(^{i}Pr$_2$Dt^0)$_2$][PF$_6$] (200 mg, 0.26 mmol) was dissolved in 13.5 mL of acetonitrile generating a dark blue solution. A solution of quinoxalinedithiol (56 mg, 0.29 mmol) and triethylamine (59 mg, 0.58 mmol) in 4.5 mL of methanol was added dropwise to the dark blue solution initiating an instantaneous color change to dark purple. The reaction mixture was stirred for one hour. The solution was filtered and green solid was collected. The green solid was washed with CH$_3$Cl to collect a dark purple filtrate. The solvent was dried en vacuo to obtain analytically pure complex. Yield 34% (49 mg, 0.091 mmol). Calcd (Expt) for C$_{18}$H$_{22}$MoN$_4$OS$_4$ + CH$_3$Cl: C, 40.27 (39.77): H, 4.63 (4.52); N, 9.89 (9.16). ^{1}H NMR (CD$_3$CN): δ 1.27(d, J= 6.7 Hz, CH$_3$, 6H), 1.41 (d, J= 6.7 Hz, CH$_3$, 6H), 3.63 (m, CH$_2$, 2H), 3.87 (m, CH$_2$, 2H), 5.25 (h, J= 6.7 Hz, CH,

2H), 7.54 (dd, $J= 6.4$ Hz, 3.4 Hz, aromatic, 2H), 7.98 (dd, $J= 6.3$ Hz, 3.4 Hz, aromatic, 2H). FTIR (KBr, cm^{-1}): 1491 (vs, C(-N)S), 1351 (vs, C=S), 950 (s, Mo=O). UV-Vis (MeCN): λ_{max} (ε, M^{-1}cm^{-1}) 400 nm (8240), 543 nm (7070).

MoO(bdtCl$_2$)(^{i}Pr$_2$Dt^0) (8). [MoOCl(^{i}Pr$_2$Dt^0)$_2$][PF$_6$] (200 mg, 0.26 mmol) was dissolved in 13.5 mL of acetonitrile generating a dark blue solution. A solution of 3,6-dichloro-1,2-benzenedithiol (61 mg, 0.29 mmol) and triethylamine (59 mg, 0.58 mmol) in 1.5 mL of acetonitrile was added dropwise to the dark blue solution initiating an instantaneous color change to dark purple. The reaction mixture was stirred for 15 minutes. The solution was filtered and dark purple solid was collected. The crude product was washed with cold chloroform to obtain analytically pure complex. Yield: 68% (100 mg, 0.181 mmol). Calcd (Expt) for C$_{16}$H$_{20}$Cl$_2$MoN$_2$OS$_4$: C, 34.85 (34.65): H, 3.66 (3.67); N, 5.08 (5.08). ^{1}H NMR (CD$_3$CN): δ1.31 (d, $J= 6.7$ Hz, CH$_\square$, 6H), 1.45 (d, $J= 6.7$ Hz, CH$_3$, 6H), 3.71 (m, CH$_2$, 2H), 4.01 (m, CH$_2$, 2H), 5.28 (h, $J= 6.7$ Hz, CH, 2H), 7.23 (s, aromatic 2H). FTIR (KBr, cm^{-1}): 1507 (vs, C(-N)S), 1356 (vs, C=S), 939 (s, Mo=O). UV-Vis (MeCN): λ_{max} (ε, M^{-1}cm^{-1}) 390 nm (4070), 530 nm (9400).
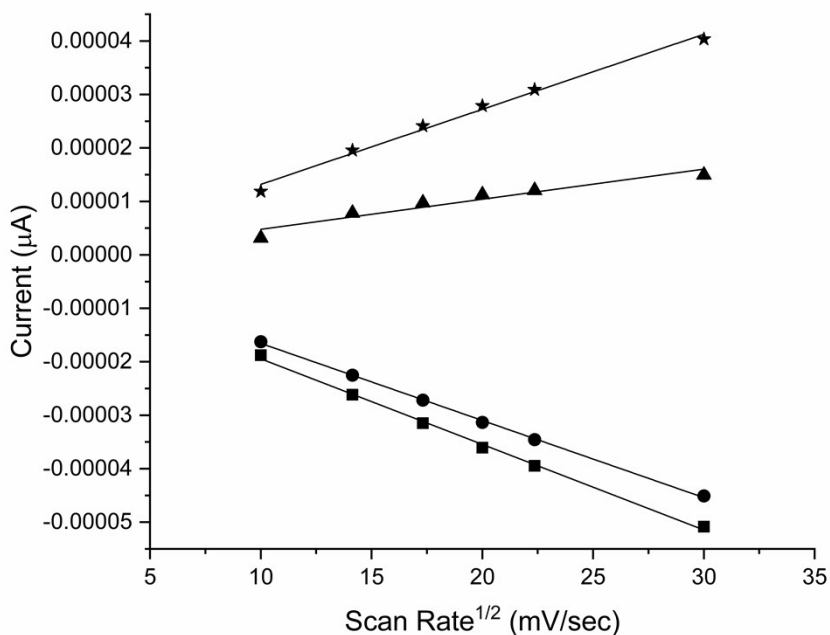
Electrochemistry

Figure S1. A plot showing the linearity of the peak current (i_p) versus the square root of the scan rate(v) for complex **6** suggesting diffusion-controlled processes. Fit of the equations are given below.

Oxidation
★ i_p= 1.40E-6(+/-6.36E-8)$n^{3/2}AD^{1/2}C^b$ -8.71E-7(+/-1.27E-6); r^2=0.99
▲ i_p= 5.63E-7 (+/-7.84E-8) $n^{3/2}AD^{1/2}C^b$ -8.56E-7 (+/- 1.57E-6); r^2=0.93
Reduction
● i_p= -1.44E-6 (+/- 1.91 E-8) $n^{3/2}AD^{1/2}C^b$ – 2.12E-6 (+/- 3.82E-7); r^2= 0.99
■ i_p= -1.60E-6 (+/- 3.78E-8) $n^{3/2}AD^{1/2}C^b$ – 3.44E-6 (+/- 7.56E-7); r^2= 0.99
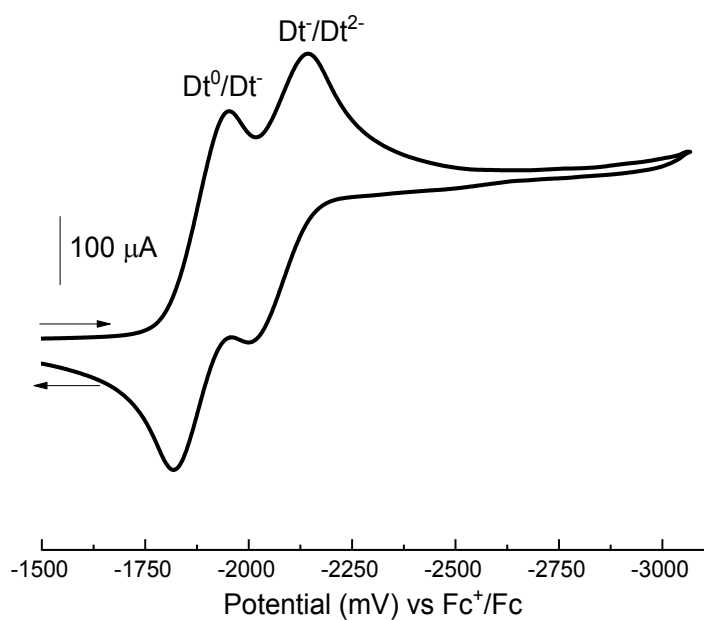
Figure S2 Cyclic voltammogram of $^iPr_2Dt^0$. Scan rate, 100mV s^{-1}; solvent, acetonitrile; temperature, 25°C; Glassy carbon working electrode, Ag/Ag$^+$ reference electrode, and a Pt-wire auxiliary electrode; supporting electrolyte, $^tBuNPF_6$. Potentials referenced internally to Fc$^+$/Fc couple.

Figure S3. Cyclic voltammogram of Zn(mnt)(^{i}Pr$_2$Dt^0) at varying scan rates ; solvent, acetonitrile; temperature, 25°C; Platinum disk working electrode, Ag/Ag$^+$ reference electrode, and a Pt-wire auxiliary electrode; supporting electrolyte, Bu$_4$NPF$_6$. Potentials referenced internally to Fc$^+$/Fc couple. 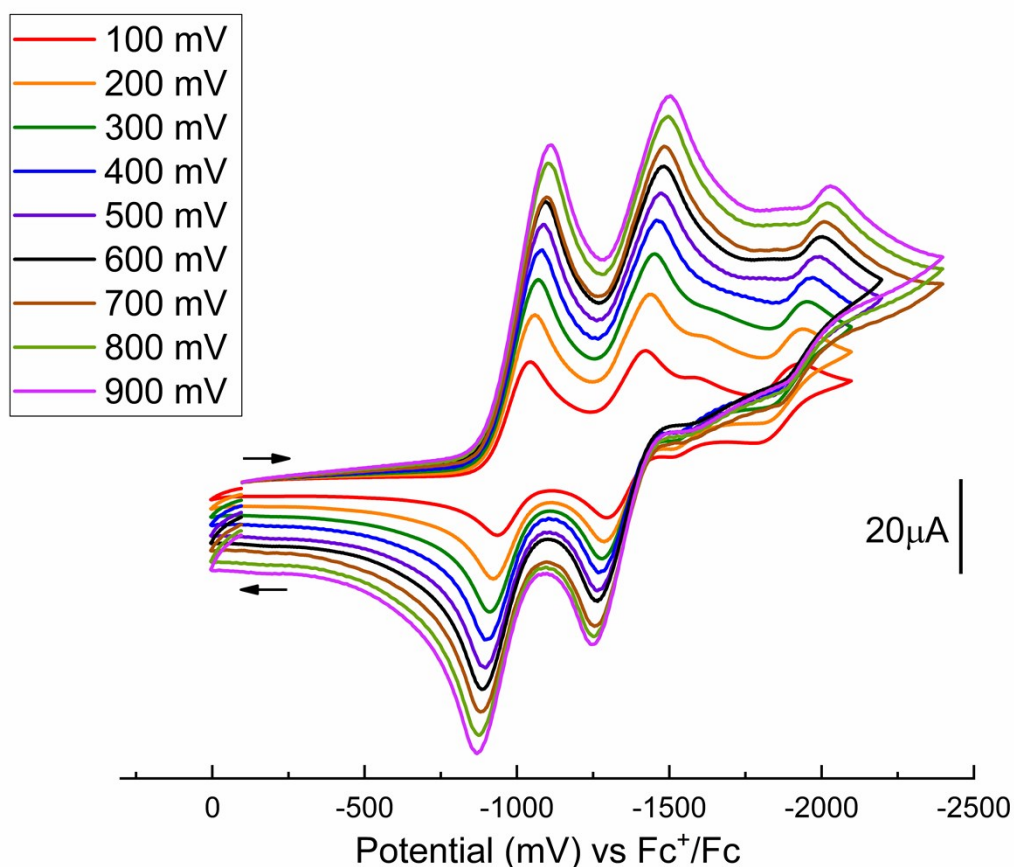The two poorly defined couples are due to potential dissociation of the ^{i}Pr$_2$Dt^0 ligand. Support for this suggestion comes from multiple scan rate experiment. As scan rate increases, the couple at E$_{1/2}$ = -1556 mV (ΔE$_p$= 90 mV) is no longer observed. The peak height of the two reversible couples attributed to the coordinated ligand increase with increasing scan rate whereas the peak heights of the couple at E$_{1/2}$ = -1556 mV (ΔE$_p$= 90 mV) does not increase. At a scan rate of 100 mV/sec the peak heights -1923 mV is ~50% and at a scan rate of 900 mV/sec the peak height at -1923 mV is ~8% of the peak height at -1601 mV. Dissociation of the ligand is a slow electron process and the concentration of free ligand can be decreased by increasing the scan rate.

Electronic Spectra
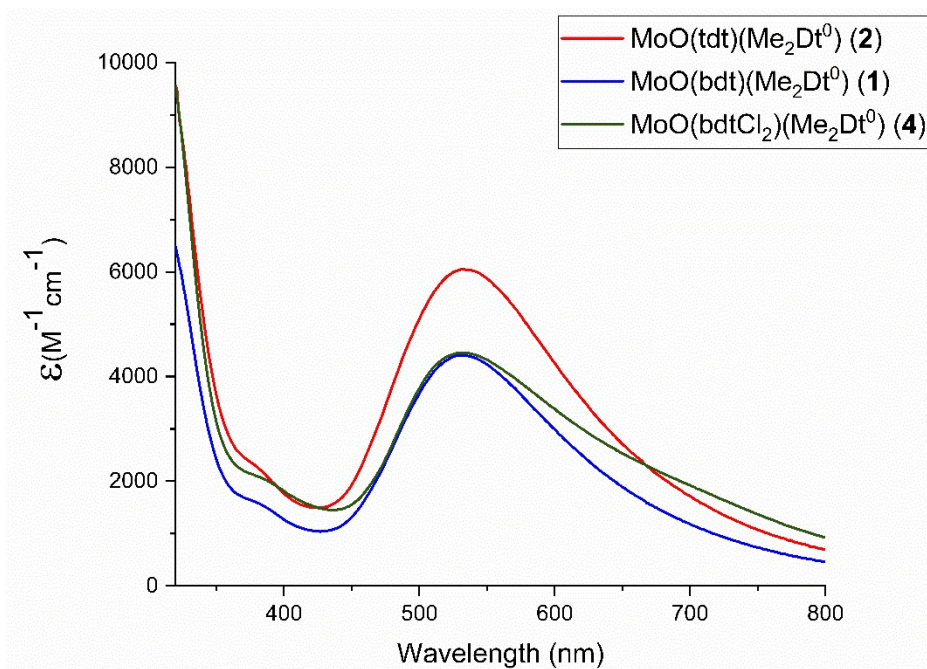
Figure S4. Absorbance spectra for complexes possessing the Me_2Dt^0 dithione ligand in acetonitrile.
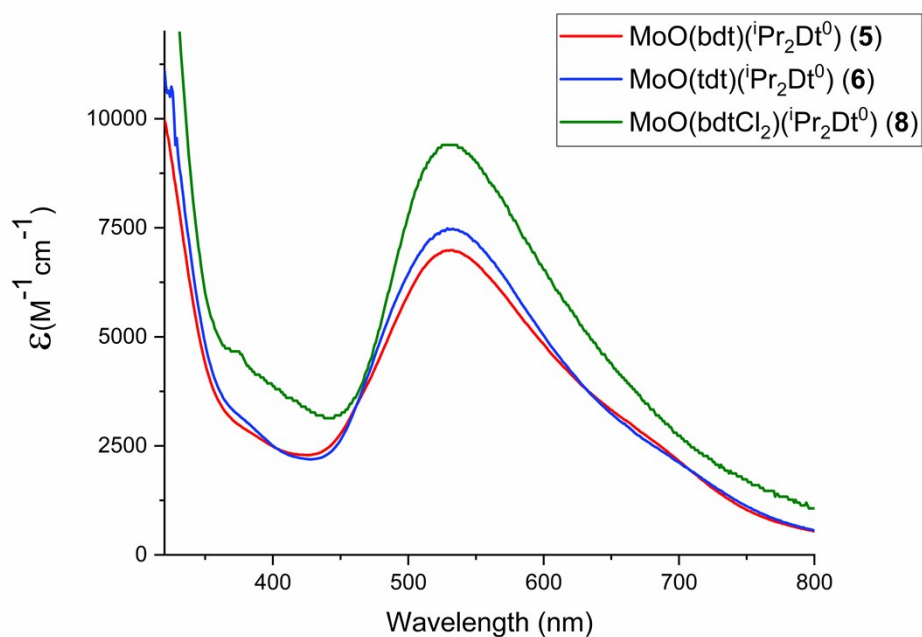
Figure S5. Absorbance spectra for complexes possessing the $^iPr_2Dt^0$ dithione ligand in acetonitrile.
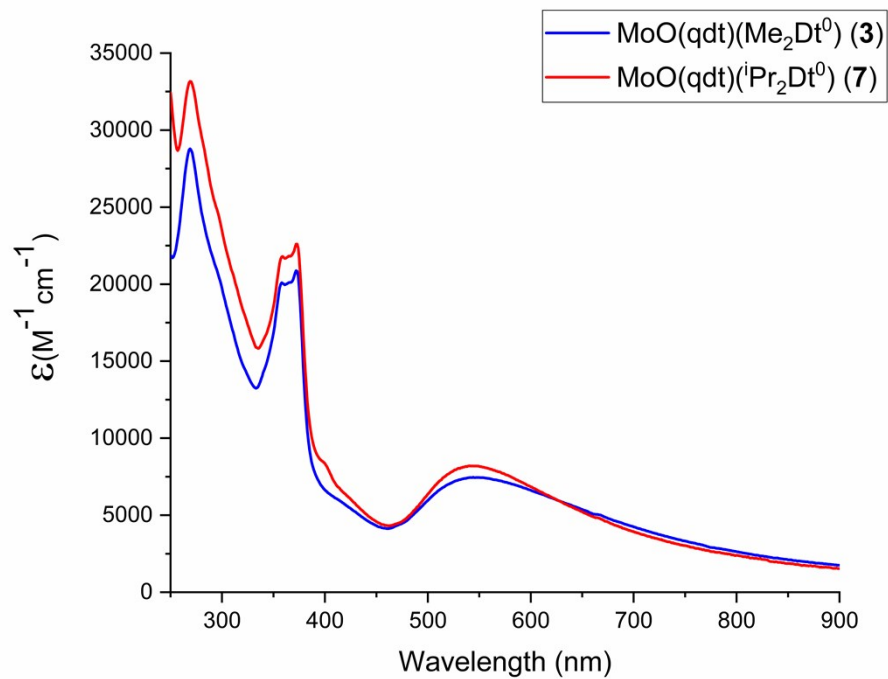
Figure S6. Absorbance spectra of **3** and **7** in acetonitrile.

Solvatochromic Effect
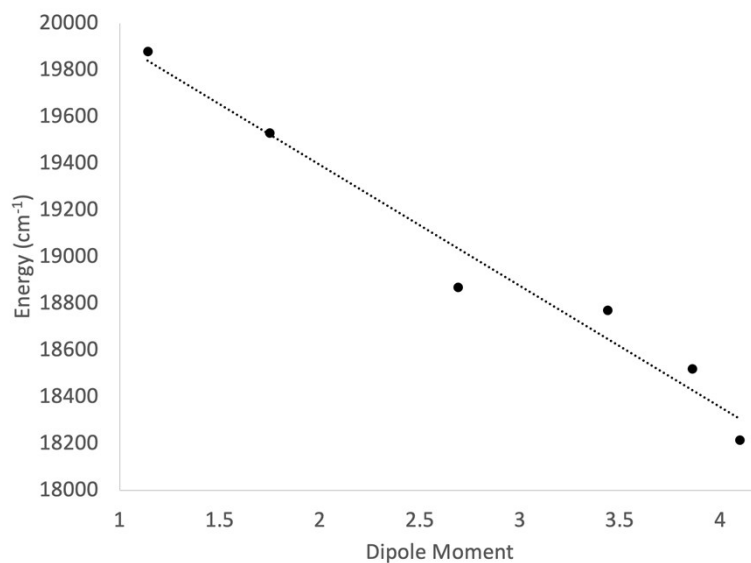
Figure S7. Linear correlation between dipole moment (μ) and the energy of the LL'CT of $MoO(bdt)(Me_2Dt^0)$. Equation of fit: $E = -518.86\mu + 20432$ $R^2 = 0.97$
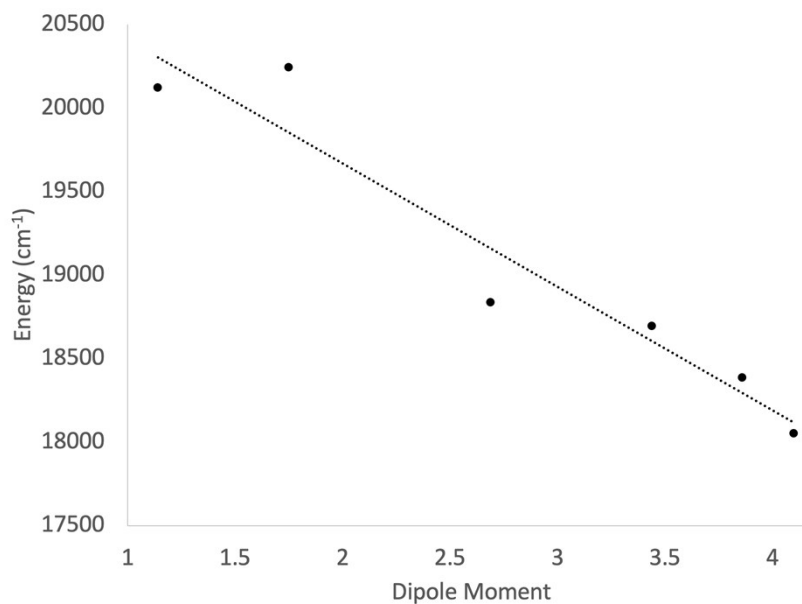
Figure S8. Linear correlation between dipole moment (μ) and the energy of the LL'CT of $MoO(tdt)(Me_2Dt^0)$. Equation of fit: $E = -739.58\ \mu + 21146$ $R^2 = 0.93$
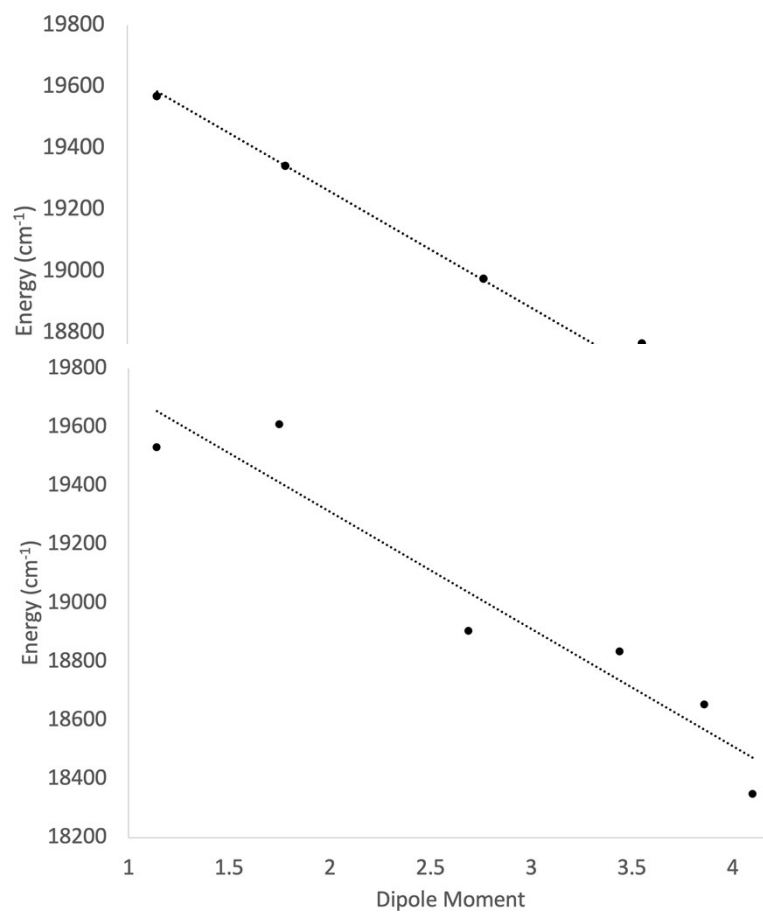
Figure S10. Linear correlation between dipole moment (μ) and the energy of the LL'CT of MoO(bdt)($^{i}Pr_2Dt^0$). Equation of fit: E = -399.03 μ + 20108 R^2 = 0.92
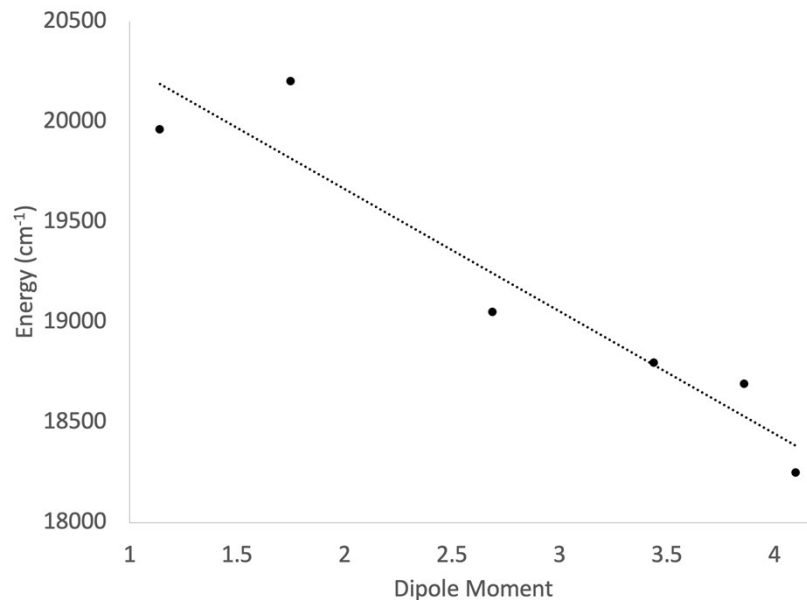
Figure S11. Linear correlation between dipole moment (μ) and the energy of the LL'CT of MoO(tdt)(^{i}Pr$_2$Dt^0). Equation of fit: E = -610.17 μ + 20884 R^2 = 0.90
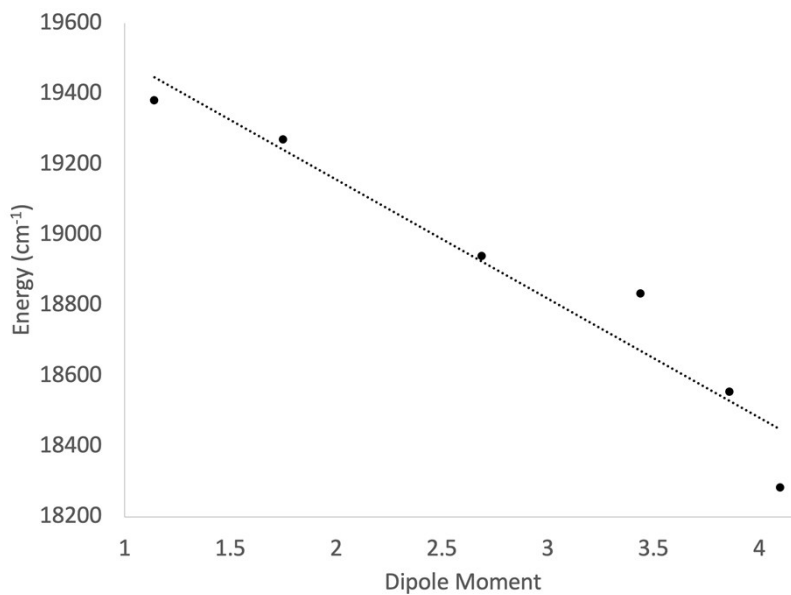
Figure S12. Linear correlation between dipole moment (μ) and the energy of the LL'CT of MoO(bdtCl$_2$)(^{i}Pr$_2$Dt^0). Equation of fit: E = -338.3 μ + 19833 R^2 = 0.93

Table S2. Composition of the molecular orbitals in **6.**

Orbital	E, eV	Mo	Mo(d)	O	tdt	S^{tdt}	$^{i}Pr_2Dt^0$	S^{Dt°
L+2	-1.05	48.47	39.81	10.24	17.89	16.34	23.40	17.21
L+1	-1.41	42.55	35.40	9.71	9.32	7.67	38.42	14.78
LUMO	**-2.81**	**25.82**	**25.37**	**1.70**	**3.08**	**1.56**	**69.40**	**22.97**
HOMO	**-4.91**	**7.46**	**4.16**	**5.63**	**82.26**	**39.79**	**4.66**	**1.60**
H-1	-5.33	1.36	1.05	1.99	87.81	49.26	8.84	6.62
H-2	-5.64	46.93	44.00	0.11	13.71	8.27	39.25	6.25

Table S3. Dt^0 fold angles ($^\circ$) of **2, 5, 6, 7,** and **8** calculated from gas phase optimizations. Compounds without crystallographic data were generated by editing **6** in *GaussView6.0* to change Dt^{2-} and Dt^0 substituents.

Complex	Dt^0 Fold Angle ($^\circ$)
$MoO(tdt)(Me_2Dt^0)$ (**2**)	65.93
$MoO(bdt)(^{i}Pr_2Dt^0)$ (**5**)	70.53
$MoO(tdt)(^{i}Pr_2Dt^0)$ (**6**)	70.47
$MoO(bdtCl_2)(^{i}Pr_2Dt^0)$ (**7**)	69.85
$MoO(qdt)(^{i}Pr_2Dt^0)$ (**8**)	69.58

Table S4. Equation of the fit for the multivariate regression using the Kamlet-Taft model.

Complex	Equation of Fit
$MoO(bdt)(Me_2Dt^0)$ (**1**)	$23726 + 1514\,\pi^* - 1675\,\alpha - 9347\,\beta$
$MoO(tdt)(Me_2Dt^0)$ (**2**)	$26752 + 1785\,\pi^* - 27025\,\alpha - 1406\,\beta$
$MoO(bdtCl_2)(Me_2Dt^0)$ (**4**)	$20777 - 3031\,\pi^* + 425.9\,\alpha + 606\,\beta$
$MoO(bdt)(^{i}Pr_2Dt^0)$ (**5**)	$23041 + 366\,\pi^* - 12720\,\alpha - 6794\,\beta$
$MoO(tdt)(^{i}Pr_2Dt^0)$ (**6**)	$25891 + 1336\,\pi^* - 23442\,\alpha - 11962\,\beta$
$MoO(bdtCl_2)(^{i}Pr_2Dt^0)$ (**8**)	$21829 - 104\,\pi^* - 7887\,\alpha - 4563\,\beta$

Table S5. Correlation coefficients of peak maxima fit to the Kamlet-Taft model.

Complex	Dipole Moment R^2	Kamlet-Taft R^2
MoO(bdt)(Me$_2$Dt^0) (**1**)	0.97	0.98
MoO(tdt)(Me$_2$Dt^0) (**2**)	0.93	0.94
MoO(bdtCl$_2$)(Me$_2$Dt^0) (**4**)	0.98	0.98
MoO(bdt)(^{i}Pr$_2$Dt$_0$) (**5**)	0.92	0.96
MoO(tdt)(^{i}Pr$_2$Dt$_0$) (**6**)	0.90	0.97
MoO(bdtCl$_2$)(^{i}Pr$_2$Dt^0) (**8**)	0.93	0.99

Theoretical Calculations

Charge = 0 Multiplicity = 1
```
Mo        -0.432   0.003    0.128
C         -3.633  -1.017    0.206
N          3.519  -1.183   -0.197
S         -2.028  -1.772    0.311
O         -0.02    0.464    1.72
S         -2.327   1.303   -0.534
C         -3.764   0.33    -0.151
N          2.922   1.551    0.052
C         -5.04    0.908   -0.239
H         -5.126   1.955   -0.517
S          0.967  -1.799   -0.81
C         -6.191   0.164    0.024
S          0.729   1.37    -1.528
C         -6.045  -1.188    0.377
C          3.845  -2.633   -0.168
H          3.062  -3.121   -0.75
C         -4.786  -1.772    0.468
H         -4.687  -2.819    0.742
C          3.953   3.772   -0.375
H          3.752   4.848   -0.362
H          4.174   3.479   -1.405
H          4.849   3.604    0.234
```

```
C        3.784   -3.177   1.265
H        2.8     -2.998   1.705
H        4.545   -2.722   1.909
H        3.964   -4.256   1.257
C        4.544   -0.243   0.263
H        5.153    0.109  -0.58
H        5.203   -0.763   0.962
C        2.73     3.02    0.162
H        1.882    3.246  -0.483
C        2.049    0.731  -0.597
C        2.355    3.419   1.596
H        2.097    4.482   1.619
H        3.183    3.269   2.299
H        1.49     2.846   1.943
C        3.878    0.927   0.964
H        3.373    0.586   1.878
H        4.633    1.663   1.243
C        5.184   -2.907  -0.862
H        5.193   -2.502  -1.878
H        5.335   -3.989  -0.927
H        6.036   -2.493  -0.314
C        2.296   -0.727  -0.549
C       -7.562    0.795  -0.059
H       -8.049    0.825   0.924
H       -8.224    0.23   -0.726
H       -7.508    1.821  -0.433
H       -6.928   -1.788   0.585
```

Excitation energies and oscillator strengths:

Excited State   1:   Singlet-A   1.9465 eV 636.95 nm f=0.0115 <S**2>=0.000
    113 ->114   0.70049
This state for optimization and/or second-order correction.
Total Energy, E(TD-HF/TD-KS) = -2507.39909459
Copying the excited state density for this state as the 1-particle RhoCI density.

Excited State   2:   Singlet-A   2.3850 eV 519.84 nm f=0.0091 <S**2>=0.000
    111 ->114   0.62758
    112 ->114   -0.30273

Excited State   3:   Singlet-A   2.4944 eV 497.06 nm f=0.1752 <S**2>=0.000
    111 ->114   0.30744
    112 ->114   0.56780
    112 ->115   -0.14893
    112 ->116   -0.17355

Excited State   4:   Singlet-A   2.8406 eV 436.47 nm f=0.0146 <S**2>=0.000
  112 ->114   0.10439
  112 ->115   0.56066
  112 ->116   -0.15536
  113 ->115   -0.33777

Excited State   5:   Singlet-A   3.0308 eV 409.08 nm f=0.0034 <S**2>=0.000
  112 ->115   0.33978
  113 ->115   0.59747

Excited State   6:   Singlet-A   3.0657 eV 404.43 nm f=0.0046 <S**2>=0.000
  109 ->114   0.17121
  110 ->114   0.64063
  112 ->116   0.18533

Excited State   7:   Singlet-A   3.2085 eV 386.43 nm f=0.1255 <S**2>=0.000
  110 ->114   -0.18069
  112 ->114   0.22461
  112 ->115   0.11939
  112 ->116   0.54462
  113 ->116   -0.25749

Excited State   8:   Singlet-A   3.3153 eV 373.98 nm f=0.0232 <S**2>=0.000
  111 ->115   0.15594
  112 ->116   0.28653
  113 ->116   0.61029

Excited State   9:   Singlet-A   3.4525 eV 359.11 nm f=0.0056 <S**2>=0.000
  109 ->114   0.12833
  112 ->117   0.55843
  112 ->118   0.24788
  113 ->117   -0.26725

Excited State 10:   Singlet-A   3.4706 eV 357.25 nm f=0.0032 <S**2>=0.000
  109 ->114   0.66222
  110 ->114   -0.17874

Excited State 11:   Singlet-A   3.5612 eV 348.15 nm f=0.0651 <S**2>=0.000
  111 ->115   0.64750
  113 ->116   -0.10787
  113 ->117   0.14787

Excited State 12:   Singlet-A   3.6969 eV 335.37 nm f=0.0319 <S**2>=0.000
  111 ->115   -0.11913
  111 ->116   -0.18849
  112 ->117   0.24848

```
    112 ->118        0.11893
    113 ->117        0.56256
    113 ->118        0.17253

Excited State  13:    Singlet-A    3.8104 eV 325.39 nm  f=0.0194  <S**2>=0.000
    105 ->114       -0.17815
    107 ->114        0.53624
    111 ->116        0.37740

Excited State  14:    Singlet-A    3.8181 eV 324.73 nm  f=0.0181  <S**2>=0.000
    105 ->114        0.12181
    107 ->114       -0.36016
    111 ->116        0.53083
    113 ->117        0.14213
    113 ->118        0.16120

Excited State  15:    Singlet-A    3.9125 eV 316.89 nm  f=0.0544  <S**2>=0.000
    108 ->114       -0.10789
    112 ->117       -0.22713
    112 ->118        0.50035
    113 ->117        0.11114
    113 ->118       -0.32321

Excited State  16:    Singlet-A    3.9883 eV 310.87 nm  f=0.0213  <S**2>=0.000
    106 ->114       -0.31306
    108 ->114        0.55191
    110 ->115       -0.16152
    112 ->118        0.18408

Excited State  17:    Singlet-A    4.0079 eV 309.35 nm  f=0.0178  <S**2>=0.000
    106 ->114        0.51169
    108 ->114        0.39698
    110 ->115        0.17722
    112 ->118       -0.10505

Excited State  18:    Singlet-A    4.0864 eV 303.40 nm  f=0.0936  <S**2>=0.000
    106 ->114        0.13289
    110 ->115        0.11047
    111 ->117        0.11717
    112 ->117       -0.12638
    112 ->118        0.27889
    113 ->117       -0.16113
    113 ->118        0.52994

Excited State  19:    Singlet-A    4.1768 eV 296.84 nm  f=0.0248  <S**2>=0.000
    111 ->117        0.65572
```

```
    111 ->118        0.12423


Excited State  20:       Singlet-A      4.2372 eV 292.61 nm  f=0.0116  <S**2>=0.000
    104 ->114        0.21900
    106 ->114       -0.20315
    110 ->115        0.59258


Excited State  21:       Singlet-A      4.3018 eV 288.21 nm  f=0.0041  <S**2>=0.000
    103 ->114       -0.11423
    104 ->114       -0.12329
    105 ->114        0.61661
    106 ->114       -0.11980
    107 ->114        0.24420


Excited State  22:       Singlet-A      4.3662 eV 283.97 nm  f=0.0326  <S**2>=0.000
    104 ->114        0.62972
    105 ->114        0.15770
    106 ->114        0.13554
    110 ->115       -0.16634


Excited State  23:       Singlet-A      4.4504 eV 278.59 nm  f=0.0073  <S**2>=0.000
    109 ->115        0.13758
    110 ->116        0.67425


Excited State  24:       Singlet-A      4.4871 eV 276.31 nm  f=0.0033  <S**2>=0.000
    111 ->117       -0.11582
    111 ->118        0.64608
    113 ->119       -0.12271


Excited State  25:       Singlet-A      4.5981 eV 269.64 nm  f=0.0558  <S**2>=0.000
    103 ->114        0.56617
    105 ->114        0.14260
    107 ->115        0.11061
    109 ->115        0.24862
    113 ->119        0.14037


Excited State  26:       Singlet-A      4.6295 eV 267.81 nm  f=0.0029  <S**2>=0.000
    103 ->114       -0.31111
    109 ->115        0.55523
    113 ->119        0.13118


Excited State  27:       Singlet-A      4.6418 eV 267.10 nm  f=0.0615  <S**2>=0.000
    109 ->115       -0.14256
    111 ->118        0.10484
    111 ->121        0.11979
    112 ->119       -0.10786
```

```
113 ->119        0.61608


Excited State  28:     Singlet-A     4.7577 eV 260.59 nm  f=0.0236  <S**2>=0.000
  109 ->116        0.27602
  111 ->121        0.16228
  112 ->119        0.46782
  113 ->120       -0.34471


Excited State  29:     Singlet-A     4.7731 eV 259.76 nm  f=0.0089  <S**2>=0.000
  107 ->115        0.21167
  109 ->116        0.51861
  112 ->119       -0.31514
  113 ->119       -0.10042


Excited State  30:     Singlet-A     4.8107 eV 257.73 nm  f=0.0291  <S**2>=0.000
  109 ->116        0.27787
  111 ->119        0.10900
  111 ->121       -0.20458
  112 ->119        0.21631
  113 ->119        0.14494
  113 ->120        0.47616
  113 ->121       -0.12391


Excited State  31:     Singlet-A     4.8633 eV 254.94 nm  f=0.0077  <S**2>=0.000
  105 ->115       -0.11500
  106 ->115        0.34877
  107 ->115        0.49262
  107 ->116       -0.14406
  112 ->119        0.13687
  113 ->121        0.11561


Excited State  32:     Singlet-A     4.8841 eV 253.85 nm  f=0.0383  <S**2>=0.000
  110 ->117        0.67121
  112 ->119        0.11108


Excited State  33:     Singlet-A     5.0164 eV 247.16 nm  f=0.0154  <S**2>=0.000
  105 ->115        0.15455
  106 ->115        0.50334
  107 ->115       -0.22939
  108 ->115       -0.30955


Excited State  34:     Singlet-A     5.0802 eV 244.05 nm  f=0.0153  <S**2>=0.000
  110 ->118       -0.15050
  111 ->119        0.52546
  113 ->121       -0.34854
```

Excited State 35:   Singlet-A   5.1479 eV 240.85 nm f=0.0589 <S**2>=0.000
  106 ->115   0.23033
  107 ->115   -0.14084
  108 ->115   0.45922
  110 ->118   -0.22321
  111 ->119   0.10786
  113 ->121   0.27042

Excited State 36:   Singlet-A   5.1506 eV 240.72 nm f=0.0061 <S**2>=0.000
  106 ->115   0.14635
  106 ->116   -0.17265
  108 ->115   0.23890
  109 ->118   0.11669
  110 ->118   0.56891

Excited State 37:   Singlet-A   5.2094 eV 238.00 nm f=0.0348 <S**2>=0.000
  106 ->116   0.30341
  107 ->116   0.31467
  108 ->115   0.11999
  108 ->116   -0.12356
  109 ->115   -0.11319
  109 ->117   0.36216
  111 ->119   -0.17508
  111 ->120   -0.13526
  113 ->121   -0.16640

Excited State 38:   Singlet-A   5.2194 eV 237.54 nm f=0.0081 <S**2>=0.000
  106 ->116   0.15554
  107 ->116   0.10114
  108 ->115   -0.25468
  109 ->117   0.20857
  110 ->118   0.20906
  111 ->119   0.31816
  111 ->120   0.17045
  112 ->120   -0.12246
  112 ->121   -0.10969
  113 ->121   0.30144

Excited State 39:   Singlet-A   5.2623 eV 235.61 nm f=0.0072 <S**2>=0.000
  107 ->116   0.11426
  108 ->116   0.11285
  109 ->117   0.13057
  111 ->120   0.10582
  112 ->119   -0.12338
  112 ->120   0.60004
  113 ->120   -0.10003

```
Excited State  40:     Singlet-A    5.2988 eV 233.99 nm  f=0.0160  <S**2>=0.000
     104 ->115       0.15956
     105 ->116       0.15174
     106 ->116       0.42719
     107 ->116      -0.27396
     108 ->116      -0.29159
     109 ->117      -0.13034
     110 ->118       0.11539
     112 ->120       0.18514

Excited State  41:     Singlet-A    5.3569 eV 231.45 nm  f=0.0043  <S**2>=0.000
     106 ->116       0.23066
     108 ->116       0.32084
     111 ->120       0.20483
     112 ->120      -0.10581
     112 ->121       0.48865

Excited State  42:     Singlet-A    5.3827 eV 230.34 nm  f=0.0046  <S**2>=0.000
     106 ->116       0.19008
     107 ->117      -0.11211
     108 ->116       0.47604
     112 ->121      -0.39969

Excited State  43:     Singlet-A    5.4083 eV 229.25 nm  f=0.1751  <S**2>=0.000
     104 ->115       0.38268
     105 ->115       0.10464
     106 ->116      -0.16401
     107 ->116      -0.17642
     107 ->117      -0.11803
     109 ->117       0.31810
     109 ->118      -0.28836

Excited State  44:     Singlet-A    5.4326 eV 228.22 nm  f=0.0101  <S**2>=0.000
     102 ->114       0.16363
     105 ->115       0.57934
     107 ->115       0.20014
     109 ->117      -0.11005
     111 ->120      -0.11958

Excited State  45:     Singlet-A    5.4489 eV 227.54 nm  f=0.0006  <S**2>=0.000
     102 ->114       0.64540
     105 ->115      -0.12692
     111 ->120       0.16194

Excited State  46:     Singlet-A    5.4807 eV 226.22 nm  f=0.0124  <S**2>=0.000
```

```
100 ->114      -0.23961
101 ->114       0.19987
102 ->114       0.13808
103 ->115      -0.10328
104 ->115      -0.19897
109 ->118      -0.18857
111 ->120      -0.10507
111 ->121       0.16781
113 ->122       0.43012
```

Excited State 47:   Singlet-A   5.5015 eV 225.37 nm f=0.0621 <S**2>=0.000
```
100 ->114       0.23975
101 ->114      -0.17767
103 ->115       0.12739
106 ->117      -0.10970
107 ->116       0.16829
109 ->118       0.13177
111 ->120       0.21300
111 ->121       0.10324
112 ->122      -0.10107
113 ->122       0.42764
```

Excited State 48:   Singlet-A   5.5346 eV 224.02 nm f=0.0222 <S**2>=0.000
```
104 ->115      -0.26849
105 ->115       0.16586
107 ->117      -0.22299
108 ->116      -0.11954
111 ->120       0.41425
112 ->121      -0.14051
113 ->121      -0.13108
113 ->122      -0.11303
113 ->123       0.10605
```

Excited State 49:   Singlet-A   5.5548 eV 223.20 nm f=0.0278 <S**2>=0.000
```
100 ->114      -0.24516
101 ->114       0.29052
104 ->115       0.34898
107 ->116       0.10953
107 ->117       0.12770
110 ->119      -0.14344
111 ->120       0.24071
113 ->121      -0.10523
```

Excited State 50:   Singlet-A   5.5971 eV 221.52 nm f=0.3068 <S**2>=0.000
```
105 ->116      -0.23973
107 ->117       0.16790
```

```
110 ->119      0.15418
111 ->121      0.34851
113 ->120      0.15887
113 ->122      -0.13031
113 ->123      0.38273
```

Excited State 51:   Singlet-A   5.6245 eV 220.44 nm f=0.0377 <S**2>=0.000

```
105 ->116      0.27856
107 ->117      0.25760
110 ->119      0.25134
111 ->121      -0.19794
112 ->122      -0.16703
113 ->120      -0.10374
113 ->122      0.11229
113 ->123      0.29587
113 ->124      0.21572
```

Excited State 52:   Singlet-A   5.6343 eV 220.05 nm f=0.0832 <S**2>=0.000

```
103 ->115      -0.13358
105 ->116      -0.10829
107 ->117      0.19326
110 ->119      0.43097
111 ->120      0.10085
113 ->123      -0.37643
113 ->124      -0.15653
```

Excited State 53:   Singlet-A   5.6411 eV 219.79 nm f=0.3031 <S**2>=0.000

```
103 ->115      -0.13789
105 ->116      0.22921
109 ->117      0.16348
109 ->118      0.37368
111 ->121      0.13076
112 ->122      0.28176
112 ->125      -0.10729
113 ->122      0.10099
113 ->124      0.21434
```

Excited State 54:   Singlet-A   5.6804 eV 218.27 nm f=0.0302 <S**2>=0.000

```
104 ->116      0.19742
105 ->116      0.27118
107 ->116      0.11384
107 ->117      0.16546
109 ->118      -0.20397
112 ->122      0.35766
113 ->124      -0.32231
```

Excited State 55:   Singlet-A   5.6932 eV 217.77 nm f=0.1248 <S**2>=0.000
  101 ->114   0.13860
  103 ->115   -0.12258
  104 ->116   0.21958
  105 ->116   0.14729
  106 ->117   -0.19196
  106 ->118   0.11019
  107 ->117   -0.14419
  107 ->118   0.13816
  108 ->117   0.24140
  109 ->118   0.17675
  111 ->121   0.13873
  112 ->122   -0.15132
  113 ->122   -0.11436
  113 ->123   0.13431
  113 ->124   -0.20188

Excited State 56:   Singlet-A   5.7106 eV 217.11 nm f=0.0709 <S**2>=0.000
  104 ->116   -0.18794
  105 ->116   0.23858
  106 ->117   0.39136
  107 ->117   -0.14292
  108 ->117   -0.16357
  110 ->119   0.13909
  112 ->122   -0.21471
  113 ->124   -0.22602

Excited State 57:   Singlet-A   5.7214 eV 216.70 nm f=0.0515 <S**2>=0.000
  101 ->114   0.19353
  103 ->115   0.19094
  104 ->116   0.43783
  106 ->117   0.17131
  108 ->117   -0.22790
  110 ->119   0.15879
  113 ->123   -0.10885
  113 ->124   0.19923

Excited State 58:   Singlet-A   5.7396 eV 216.01 nm f=0.0513 <S**2>=0.000
   99 ->114   0.13143
  100 ->114   0.24059
  101 ->114   0.29713
  103 ->115   0.23650
  104 ->116   -0.24899
  107 ->117   -0.12148
  110 ->119   0.16992
  112 ->122   0.23811

Excited State 59:   Singlet-A   5.7444 eV 215.84 nm f=0.1251 <S**2>=0.000
   99 ->114   0.20373
  100 ->114   0.37849
  101 ->114   0.23903
  103 ->115   -0.25745
  106 ->118   -0.12772
  107 ->118   -0.12166
  110 ->119   -0.14531
  111 ->121   0.14409
  112 ->122   -0.10573
  113 ->123   -0.11229

Excited State 60:   Singlet-A   5.7640 eV 215.10 nm f=0.0240 <S**2>=0.000
  103 ->115   0.29635
  106 ->117   0.16461
  108 ->117   0.46809
  108 ->118   0.13178
  111 ->121   0.15247
  113 ->123   -0.12717
  113 ->124   0.17370